stellarator news

Published by Fusion Energy Division, Oak Ridge National Laboratory
Building 9201-2 P.O. Box 2009 Oak Ridge, TN 37831-8071, USA

Editor: James A. Rome Issue 44 March 1996
E-Mail: jar@ornl.gov Phone: (423) 574-1306 Fax: (423) 574-0680

Reorganization of the Kyoto University Plasma Physics Laboratory

The Japanese government has unofficially approved the establishment of the Graduate School of Energy Science and the Institute of Advanced Energy at Kyoto University (Kyoto, Japan), as proposed in the Ministry of Education (Monbusho) budget plan for fiscal year 1996. Following official approval by the Diet, which is expected this month, these two organizations will commence operations in April. The Plasma Physics Laboratory will be reorganized so that it can participate in these two organizations.

The Graduate School of Energy Science is to be composed of several chairs from the present Faculties of Engineering, Science, Agriculture, and Economics; sections from the present Institute of Atomic Energy; and the Plasma Physics Laboratory. The major purpose of the Graduate School of Energy Science is to provide students with a wide range of knowledge and ability concerning global energy science, focusing not only on engineering aspects, but also on interdisciplinary sciences such as energy development and utilization management and economic and environmental problems.

The Institute of Advanced Energy is to becomposed of sections from the Institute of Atomic Energy and the Plasma Physics Laboratory. The new Institute will be devoted mainly to research on the physical and technological aspects of advanced energy science in cooperation with the Graduate School of Energy Science.

The role of the present Heliotron group in the new organizations apparently will be to educate successors and specialists in fundamental fusion science and related fields as a part of “global” energy science. The goal is to contribute to the development of fusion science and technology from the viewpoint of advanced energy research by keeping in close contact with and providing mutual support for the National Institute for Fusion Science (NIFS) project.

Operation of the Heliotron E device will be continued at the new institute until the start of the LHD experiment. The plan after the end of the Heliotron E experiment is under consideration. The next machine should then be constructed to support the advanced energy programs described above.

We hope to broaden our program and to increase cooperation with all stellarator groups in the world. We welcome any questions, comments, and suggestions.

Tokuhiro Obiki, Director
Plasma Physics Laboratory
Kyoto University
611 Uji, Kyoto, Japan

E-mail: obiki@ppl.kyoto-u.ac.jp
Voice: 81-774-32-9392
FAX: 81-774-32-9397

In this issue . . .

Resonant and nonresonant electron cyclotron heating (ECH) at densities above the plasma cut-off by O-X-B mode conversion

The O-X-B mode conversion process was proposed by Preinhaelter and Kopecký [1] in 1973 as a possibile means of overcoming the density limit for electron cyclotron resonance heating (ECRH). Here O, X, and B represent the O-mode, X-mode and electron Bernstein mode. The essential part of this scheme is the conversion of the O-wave launched by an antenna from the low field side into an X-wave at the O-wave cut-off layer. This mode conversion requires the O-wave to be injected near an optimal angle oblique to the magnetic field.

As shown in Fig.1 the square of the transverse refractive index N_x^2 of the O-wave and N_x^2 of the X-wave are connected at the optimal launch angle with a corresponding longitudinal (parallel B_0) index $N_{z,\mathrm{opt}} = [Y/(Y+1)]^{1/2}$, with $Y = \omega_{ce}/\omega$ (ω is the wave frequency, ω_{ce} is the electron cyclotron frequency), without passing a region of evanescence ($N_x^2 < 0$), while for nonoptimal launch an evanescent region always exists. The geometrical size of the evanescent region depends on the density scale length $L = n_e/(\partial n_e/\partial x)$, and a considerable fraction of the energy flux can be transmitted through this region, if L becomes small. Several different formulas have been derived for the transmission coefficient through the cut-off layer, using both the WKB approximation and full-wave calculations [1–3]. Note that transmission through the cut-off layer is equivalent to O-X conversion.

After the O-X conversion, the X-wave propagates back to the upper hybrid resonance (UHR) layer, where the refractive index of the X-wave is connected to that of the electron Bernstein waves (EBWs) as shown in Fig. 2, and a complete conversion into EBWs should take place. The EBWs then move towards the plasma center, where they are absorbed near the electron cyclotron resonance layer. Further theoretical investigations have been performed by Meakawa et al. [4,5] and by Hansen, Lynov, and Michelsen [6], who have carried out ray-tracing calculations for the resonant heating.

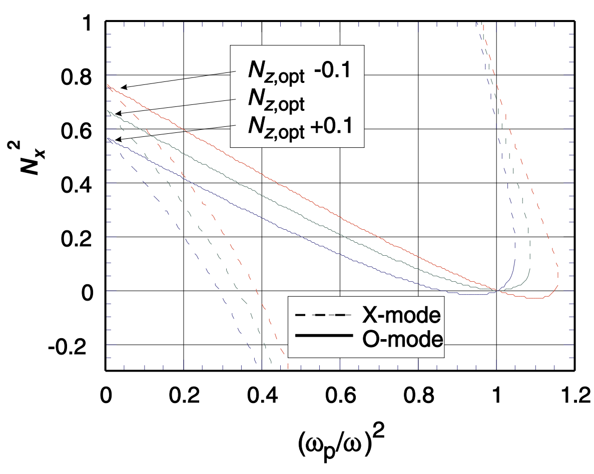

Fig. 1. Square of the refractive index N_x^2 versus $(\omega_p/\omega)^2$ for different values of N_z ($Y = 0.6$, $N_y = 0$, ω_p is the plasma frequency).

In our calculations, we also take into account that in a real plasma the conversion layer is not a smooth surface but is rough and wavy owing to density fluctuations. This introduces a beam divergence that is much higher than the intrinsic one and can drastically reduce the O-X-conversion. With a statistical description of the poloidal cut-off surface roughness (toroidal fluctuations were neglected), the probability density function

$$p(N_y) = \frac{\lambda_y}{\sqrt{2\pi}\ \sigma_x} \exp\left[-\frac{N_y^2 \lambda_y^2}{(1-N_y^2)\,2\sigma_x^2}\right](1-N_y^2)^{-3/2}$$

of the poloidal component N_y could be calculated as a function of the fluctuation amplitude standard deviation $\sigma_x = \tilde{n}_e/n_e$ ($\tilde{n}_e$ is the relative fluctuation amplitude) and the poloidal correlation length λ_y. The modified transmission function T_{mod} (O-X conversion efficiency) is then $T_{\mathrm{mod}}(N_z) = \int T(N_y,N_z)\, p(N_y) \mathrm{d}N_y$.

Here $T(N_y,N_z)$ is the transmission coefficient given by Mjøhus [2] with

$$T(N_y, N_z) = \exp\left\{-\pi k_0 L \sqrt{\frac{y}{2}}\left[2(1+y)(N_{z,opt} - N_z)^2 + N_y^2\right]\right\}$$

where N_z is the longitudinal component of the vacuum refractive index and k_0 is the wave number.

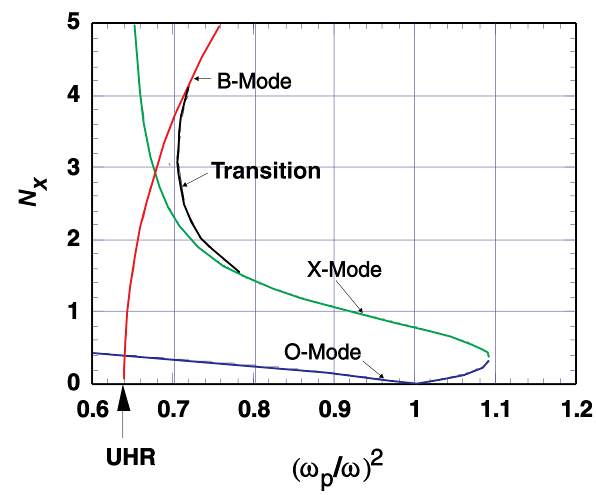

Fig. 2. Refractive index N_x versus $(\omega_p/\omega)^2$ for the O-X-B conversion process ($Y = 0.6$, $N_z = N_{z,\mathrm{opt}}$, and $N_y = 0$). The B-mode N_x was calculated for a temperature of 500 eV. The transition represents the connection of the X-mode and B-mode owing to the hot dielectric tensor.

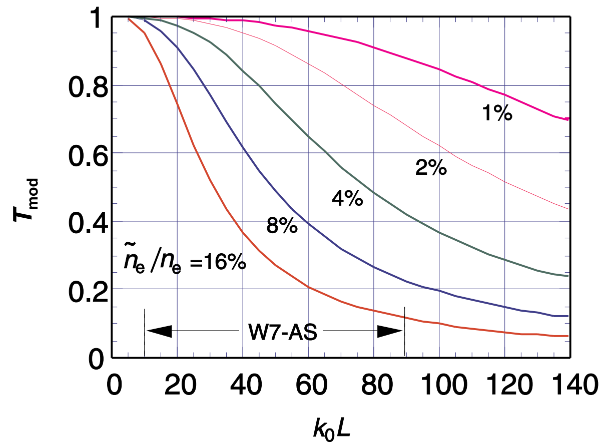

Fig. 3. Modified O-X conversion in the presence of density fluctuations at the plasma cut-off layer for different relative fluctuation amplitudes versus normalized density scale length k_0L ($N_z = N_{z,opt}$ and $Y =$ 0.6). The markers show the accessible values of k_0L on W7-AS.

In Fig. 3 the modified transmission is calculated as a function of the parameter k_0L for five relative density fluctuation amplitudes. In all calculations the poloidal correlation length was assumed to be 2 cm. It can be clearly seen that to achieve a significant heating efficiency the target plasma should have either a very small density scale length or a very low fluctuation amplitude.

The flexibility of W7-AS makes it possible to investigate two extreme cases: target plasmas with $L \leq 1$ cm but with a relative density fluctuation amplitude of more than 10%, and peaked density profiles (L = 4 cm) with a very low relative fluctuation amplitude (< 1%). For both cases, high conversion efficiencies were experimentally achieved and O-X-B mode conversion for plasma heating could be clearly shown for the first time. Two 70-GHz beams were launched into a neutral beam (NBI) sustained target plasma at resonant (1.25-T) and nonresonant (1.75-T) magnetic fields. The launch angle of the incident O-mode polarized wave was varied at fixed heating power (220 kW).

An example of the nonresonant case is shown in Fig. 4. The increase of the total stored plasma energy (from the diamagnetic signal) depends strongly on the longitudinal refractive index, which is typical for the O-X conversion process and fits well to the calculation. The central density was 1.5×10^{20} m^{-3}, which is more than twice the cut-off density, and the central electron temperature was 500 eV. Owing to technical limitations on the maximum launch angle, only the left part of the calculated reduced transmission function could be tested experimentally.

Typical for X-B conversion at the UHR layer is the parametric instability which generates waves with frequencies of the incident wave ω plus and minus the harmonics of the lower hybrid (LH) frequency ω_{LH} and the LH wave itself. With the electron cyclotron emission (ECE) receiver, a spectrum of the decay waves with maxima at $\omega \pm n\omega_{LH}$ was measured for a resonant magnetic field of 1.25 T, as shown in Fig. 5. Note that the incident frequency is excluded and that since the density was twice the 70-GHz cut-off density this could not be a thermal ECE spectrum. The low-frequency L -wave itself could be detected with a broadband loop antenna. A high degree of correlation between the high-frequency decay waves and the LH wave was measured.

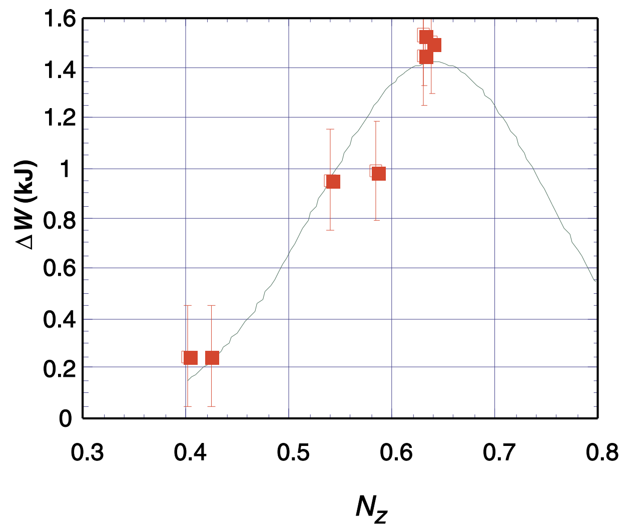

Fig. 4. Increase of the plasma energy content ΔW (squares) by O-X-B heating versus the longitudinal vacuum refractive index N_z of the incident O-wave at a magnetic field of 1.75 T and k_0L = 10. The solid line is the calculated modified transmission function $T_{mod}(N_z)$ multiplied by the maximum energy increase for $N_y = 0$.

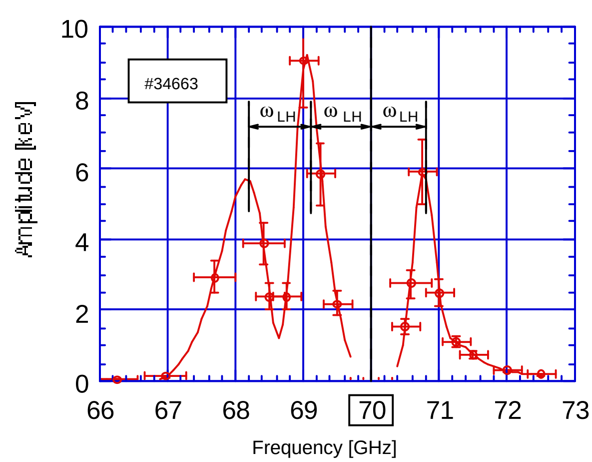

Fig. 5. High-frequency spectrum of the parametric decay waves generated in the O-X-B process. The incident wave frequency is 70 GHz, and the LH frequency is about 900 MHz.

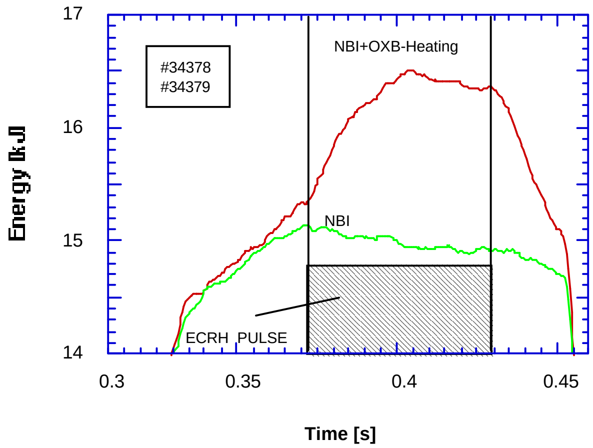

Fig. 6. Energy content (diamagnetic signal) of an NBI discharge with (upper curve) and without (lower curve) nonresonant O-X-B heating at a magnetic field of 2.0 T.

EBWs experience a cut-off layer ($N \Rightarrow 0$) at the UHR (see Fig. 2), and the radiation is trapped inside the plasma as it is in a hohlraum. The EBW is either (in the case of an oblique angle of incidence) reflected at the UHR or back converted to the X-wave, which is converted again to the EBW at its next contact with the UHR. The only way that radiation can escape from the plasma is through the small angular window for O-X and X-O conversion respectively. With no electron cyclotron resonance in the plasma, the B-waves may be absorbed because of finite plasma conductivity after some reflections at the UHR layer. Nonresonant heating was investigated at magnetic fields up to 2.0 T. At the maximum field the plasma energy content increased by about 1.5 kJ compared to an similar discharge with NBI only, as shown in Fig. 6. Two 70-GHz beams in O-mode polarization (110 kW of power each) were launched with an angle of 40° with respect to the perpendicular launch into a target plasma sustained with 800 kw of NBI, with a central density of $1.6 \times 10^{20}\,m^{-3}$ and a central temperature of 560 eV.

In conclusion, the O-X-B heating scheme with 70-GHz electron cyclotron waves was clearly demonstrated for the first time for resonant and nonresonant fields at W7-AS. Both, the angular dependence of the O-X conversion and the parametric instability which is typical for X-B conversion were experimentally verified. Density fluctuations at the O-X conversion layer play a significant rule in the O-X-B process and need to be taken into account.

With a newly developed three dimensional ray-tracing code for EB's and improved measurement techniques for determining the power deposition profiles, further investigations of the O-X-B heating are envisaged to explore the potential of resonant and nonresonant O-X-B heating for routine high-density operation.

References

[1] J. Preinhaelter and V. Kopecký, J. Plasma Phys. **10** (1973) 1.

[2] E. Mjøhus, J. Plasma Phys. **31** (1984) 7.

[3] F. R. Hansen, J. P.Lynov, C. Maroli, and V. Petrillo, J. Plasma Phys. **39** (1988) 2.

[4] T. Meakawa, S. Tanaka, Y. Terumichi, and Y. Hamada, Phys. Rev. Lett. **40** (1978) 1379.

[5] T. Meakawa, S. Tanaka, Y. Terumichi, and Y. Hamada, J. Phys. Soc. Japan **48** (1980) 247.

[6] F. R. Hansen, J. P. Lynov, and P. Michelsen, Plasma Phys. Controlled Fusion **27** (1985) 1077.

H. P. Laqua for the W7-AS Team
Max Planck Institut für Plasmaphysik
Garching bei München, Germany
E-mail: laqua@ipp-garching.mpg.de
Phone: 0049-89-3299-1742

ICRH experiments on W7-AS

Ion cyclotron resonant heating (ICRH) has been successfully demonstrated for the first time on W7-AS. A novel antenna [1] designed to excite a narrow spectrum of fast waves was used. Two different heating scenarios were investigated: second harmonic heating of neutral beam heated hydrogen plasmas and H-minority heating of electron cyclotron resonant heating (ECRH) deuterium plasmas. Both scenarios showed plasma heating without a significant concurrent increase in plasma density or impurity radiation loss. In addition, it was possible to sustain the plasma with ICRH alone.

The ICRH antenna, shown in Fig. 1, is located on the high field side of the elliptically shaped plasma. It has four feeders that allow operation in 0- and π-phasing. Typically it is operated in π-phasing. In this situation, the poloidal current has an almost sinusoidal distribution in the toroidal direction and excites a narrow $k_{\parallel} \approx 6\ \mathrm{m}^{-1}$ spectrum of fast waves. During the Spring 1995 opening of the torus vessel, the feeders to the antenna, shown in Fig. 2, were closed off against plasma penetration. This eliminated the anomalously high loading of the antenna during plasma operation that had been observed previously [2] and increased the maximum rf voltage at which electrical breakdown (arcing) occurred. Voltages of up to 55 kV for 400 ms have now been achieved after extensive conditioning. Because of the low antenna plasma loading of about $0.5\ \Omega$, the maximum power delivered to the antenna was limited to about 400 kW by arcing in the transmission lines or antenna feeders. Most plasma targets had $\bar{\iota} \sim 0.33$ and were shaped by inside limiters.

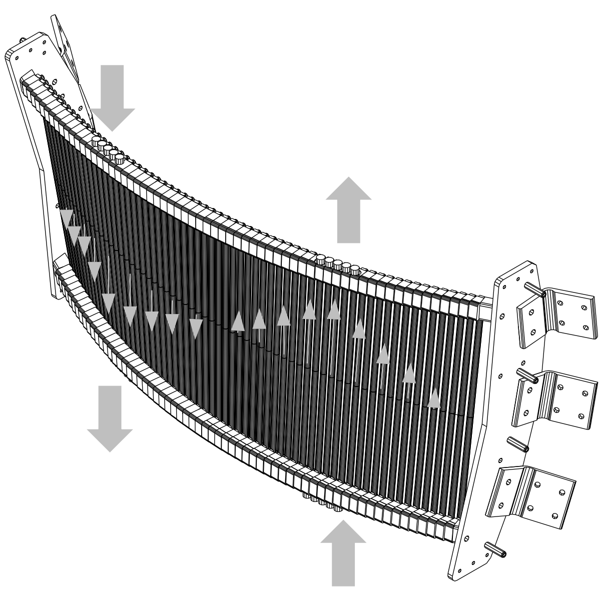

Fig. 1. ICRH antenna, shown without the Faraday screen.

The distance between the antenna and the fast wave cut-off is about 6 cm.

In the second harmonic hydrogen heating scenario with a neutral beam heated target plasma, an increase in the diamagnetic energy of about 10% (0.6 kJ) was obtained. We estimate that about 60% of the power P radiated from the antenna is found in the plasma, if P is the generator power reduced by the Ohmic losses in the antenna and $P^{-0.6}$ scaling of the energy confinement time is invoked. Under good wall conditions, the plasma density could be kept constant during the rf pulse, even though the H_{α} diagnostic in the antenna region indicated enhanced outgassing. The impurity radiation as inferred from the bolometer did not increase. An increase in the flux of hydrogen atoms with energies up to 33 keV was observed; however, no significant increase in the bulk hydrogen temperature was seen. Maximum heating occurred if the location of the second harmonic resonance coincided with the center of the plasma; almost no heating occurred if the resonance was outside the plasma.

The antenna loading was independent of the location of the resonance even though an rf probe (located halfway around the torus) detected a wave signal only if the resonance was outside the plasma. Heating at 0-phasing showed similar increases in the diamagnetic energy and no enhanced impurity radiation. No significant heating

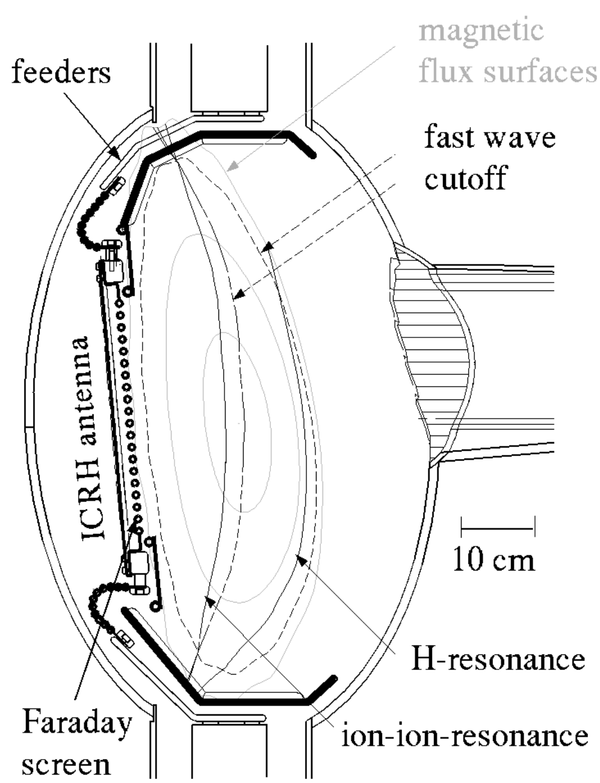

Fig. 2. Poloidal cross section through the ICRH antenna. Resonances and cut-offs are shown for the ICRH plasma of Fig. 3.

was observed in ECRH plasmas of the same density, presumably because the ion temperature of the target plasma was too low.

In the H-minority heating scenario with an ECRH target plasma, an increase in the diamagnetic energy of about 15% (1 kJ) was obtained. This corresponds to absorption of about all of the radiated power *P*. The spectroscopically estimated H/D ratio was about 10%. The line-of-sight averaged deuterium temperature rose from 300 eV to 400 eV; the central electron temperature rose slightly. Energetic hydrogen atoms with energies up to 30 keV were observed. The impurity radiation did not increase.

In the H-minority heating scenario, it was possible to sustain an ECRH-created plasma with ICRH alone. In all cases the duration of the plasmas was limited by arcing in the transmission lines. A near-steady-state condition could be obtained about 200 ms into the ICRH-only phase of the discharge. Typical parameters were diamagnetic energy of 2 kJ, average electron density of 4.0×10^{19} m^{-3}, central electron temperature of 300 eV, and central deuterium temperature of 350 eV.

An example of an ICRH-sustained plasma, starting at 400 ms, is shown in Fig. 3. The generator frequency and the approximate H/D ratio were such that both the H-resonance and the ion-ion resonance were located in the plasma, as shown in Fig. 2. The average electron density first rose because of increased outgassing of the antenna but returned towards the initial value near the end of the ICRH plasma. The central electron temperature dropped rapidly within an energy confinement time and then stayed constant throughout the ICRH phase. The total radiation measured with bolometers stayed constant, even though an accumulation of iron and chromium could be inferred from vacuum ultraviolet (VUV) observation; soft X-ray measurements however, indicated that Z_{eff} stayed constant. Thus, the ICRH plasma does not seem to be hampered by impurities.

The plasma density profile, measured with a lithium beam diagnostic, Langmuir probes, microwave reflectometry, and Thomson scattering, was narrower and had steeper edges than in comparable ECRH-heated plasmas. The transition between these two profiles occurred within approximately one energy confinement time. Further narrowing of the plasma was observed on a longer time-scale. The resulting increase in the distance from the antenna to the fast wave cutoff could explain the decrease of the antenna plasma loading and therefore the decrease in diamagnetic energy. A radial electric field of about −1.5 kV/m built up at the beginning of the ICRH phase of the discharge, presumably due to increased high-energy hydrogen losses as indicated by charge exchange (CX) measurements.

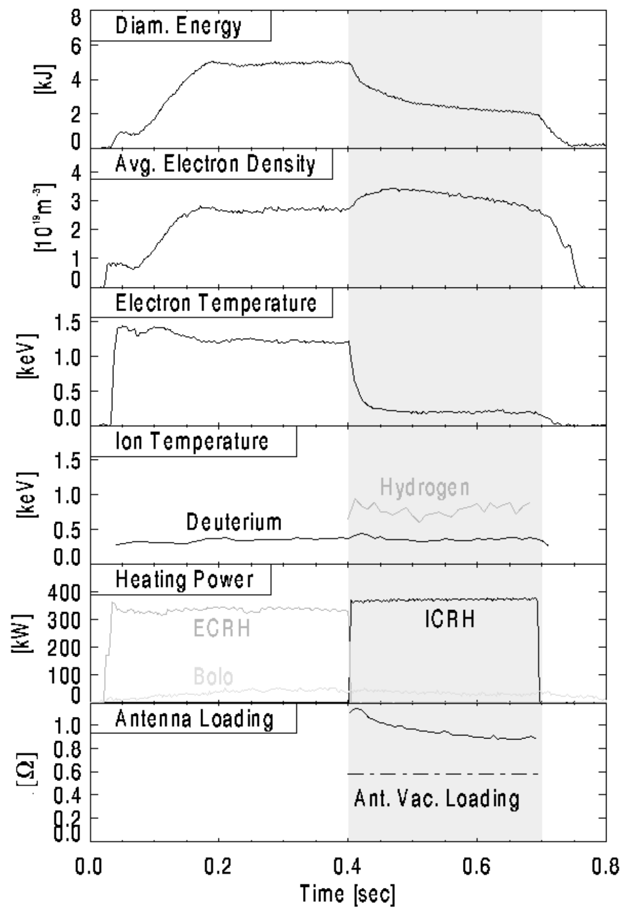

Fig. 3. Time trace of shot 33634. B_T = 2.5 T, ι = 0.34. Ion temperatures inferred from unweighted line-of-sight average of CX fluxes.

References

[1] G. Cattanei et al., *Stellarator News*, Issue 25, January 1993, p. 3.

[2] M. Ballico et al., in IAEA Technical Committee Meeting on Stellarators and Other Helical Confinement Systems, Garching (1993) 413.

Dirk Hartmann, Giorgio Cattanei for the W7-AS and ICRH Teams
IPP Garching, EURATOM Association
Garching bei München, Germany
E-mail: dih@ipp-garching.mpg.de
Voice: 0049-89-3299-1235